Eur. Phys. J. D **16**, 127–131 (2001)

THE EUROPEAN PHYSICAL JOURNAL D

EDP Sciences

Control of wavepacket dynamics in mixed alkali metal clusters by optimally shaped fs pulses

A. Bartelt[a], S. Minemoto[b], C. Lupulescu, Š. Vajda, and L. Wöste

Institut für Experimentalphysik, Freie Universität Berlin, Arnimallee 14, D-14195 Berlin, Germany

Received 4 December 2001

Abstract. We have performed adaptive feedback optimization of phase-shaped femtosecond laser pulses to control the wavepacket dynamics of small mixed alkali-metal clusters. An optimization algorithm based on Evolutionary Strategies was used to maximize the ion intensities. The optimized pulses for NaK and Na_2K converged to pulse trains consisting of numerous peaks. The timing of the elements of the pulse trains corresponds to integer and half integer numbers of the vibrational periods of the molecules, reflecting the wavepacket dynamics in their excited states.

PACS. 82.50.Nd Control of photochemical reactions – 82.33.Fg Reactions in clusters – 82.53.Eb Pump probe studies of photodissociation

1 Introduction

The dynamics of small alkali metal clusters has intensively been studied by pump-probe technique in the last decade [1]. In the transient spectra of the homo- and heteronuclear sodium and potassium dimers pronounced oscillatory structures were detected. They could be explained by the wavepacket propagation in coherently excited bound states [2]. The mixed trimer spectra, however, are almost all dominated by an exponential decay with time constants of a few ps [3,4]. This fragmentative behaviour of the excited states indicates the presence of dissociative and predissociative states. In some cases oscillations superimposed on the exponential decay were recorded, indicating the survival of coherent motions during the fragmentation. Thus an active manipulation of the photofragmentation channels acting on the wavepacket dynamics becomes possible. In the last two decades a great theoretical effort was made in order to control molecular dynamics evoked by irradiation of designed laser fields. Different schemes have been established. The concept of "coherent control" by Brumer and Shapiro drives unimolecular reactions by controling the relative phase of cw-lasers of different energy [5,6]. In the "pump-dump" approach proposed by Tannor, Kosloff and Rice [7,8] the pump pulse creates a wave packet in the excited state, which is subsequently dumped by the second pulse into the dissociation channel of the ground state potential. Optimal control theory was demonstrated by Rabitz and coworkers [9–12] to predict arbitrary pulse forms, which drive the wave packet into the desired product channel. Pulse forms were calculated in a "trial-and-error" fashion, using optimization algorithms in order to converge to the objective. With the development of computer controllable pulse shaping techniques [13] Judson and Rabitz suggested adaptive feedback optimal control (AFOC) [14]. Non-deterministic optimization algorithms were proposed to find the optimal laser field in the laboratory without any knowledge of the Hamiltonian. In first experiments by Assion *et al.* [15] photoionic product ratios in the exponential decay channels of organo-metallic complexes were optimized. An open and important question is the information content about the evoking processes being dechiffred in the optimized laser field. AFOC experiments with small mixed alkali metal clusters are presented for two reasons: First they are photo-dissociative systems, which exhibit oscillatory wavepacket features during the fragmentation. Secondly, cluster beams offer the possibility to distinguish between the fragmentation and the ionization process. If fragment ion yields are optimized, generally both processes are involved in an unknown sequence. If however, the cluster beam does not contain clusters of higher mass than the ionic product, only the ionization is optimized. These comparisons are still under way and will be given in a subsequent publication. In this paper we present adaptive feedback control of transient multiphoton ionization and fragmentation of the alkali metal clusters NaK and Na_2K by optimally phase-shaped fs pulses.

[a] e-mail: bartelt@physik.fu-berlin.de

[b] *Present address:* School of Science, The University of Tokyo, 7-3-1 Hongo Bunkyo-Ku, Tokyo 113-0033, Japan.

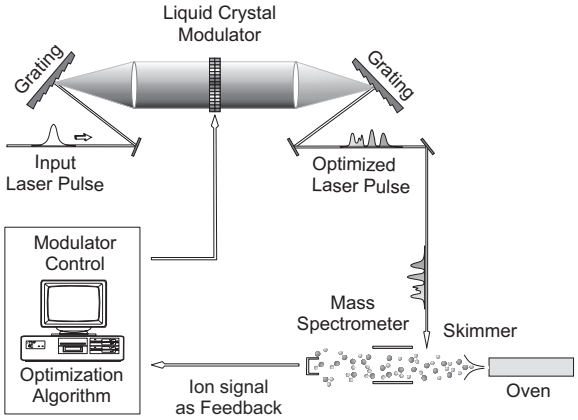

Fig. 1. Scheme of the adaptive feedback optimization setup. A selflearning algorithm controls the pulse shaper in order to maximize the ion yield.

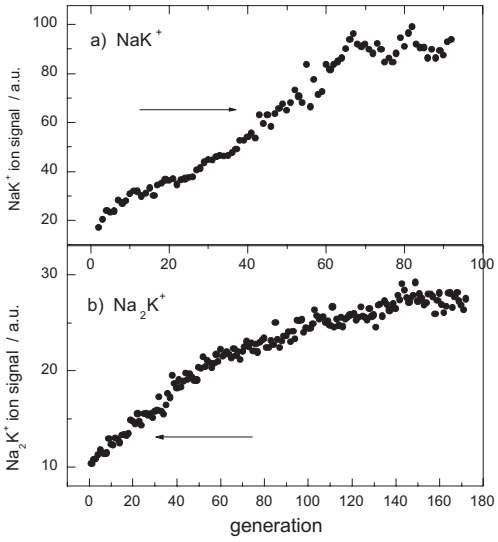

Fig. 2. Maximization of the ion yield for (a) NaK^+ and (b) Na_2K^+. The algorithm starts with random pulse forms and iteratively increases the ion yield. The arrows indicate the ion yield obtained with a transform-limited pulse of the same energy.

2 Experimental setup

The alkali metal clusters are produced in an adiabatic expansion of alkali steam through a nozzle of 70-μm diameters. The cluster size distribution depends on the alkali oven temperature and on the pressure of the argon used as carrier gas. The oven is heated to temperatures between 650 and 800 °C, and the argon pressure ranges between 2-4 bars. Details of the mixed alkaline cluster production can be seen elsewhere [16]. The alkali clusters are excited and ionized by a tunable fs laser beam and detected with a quadrupole mass spectrometer (Balzers QMG 420). We use a TiSa Oscillator (Spectra Physics 3960 Tsunami) pumped by a Nd:YLF laser (Spectra Physics Millenia X) with a repetition rate of 80.6 MHz, 1.8 W laser power and pulse durations of 80 fs at a center wavelength of 770 nm. Maximization of the ion yield is realized by shaping the form of the fs-pulses. The ion yield is taken as feedback in a non-deterministic optimization algorithm based on Evolutionary Strategies. The pulse forms presented in this paper are analyzed by intensity cross-correlation and SHG FROG [24]. To obtain phase and amplitude from the FROG trace phase retrieval algorithms based on generalized projections and genetic algorithms are used [25].

2.1 Pulse shaper

With a programmable pulse shaper system pulse forms of arbitrary temporal intensity and phase can be created [13,17,18]. The heart of the system is a spatial light modulator (SLM) consisting of 2 liquid-crystal arrays of 128 pixels each, and 2 polarizers. The SLM is placed in the Fourier plane of a linear zero dispersion compressor [19], which consists of 2 gratings (1200 l/mm), and 2 cylindrical lenses ($f = 200$ mm). The gratings disperse and recombine the spectrum of the pulse, the lenses focus the spectral components on the Fourier plane. By applying voltages on each pixel independently, variable phase shifts and attenuation of the spectral components of the pulse can be achieved. Pulses of 70 fs duration and 8.5 nm FWHM at a central wavelength of 770 nm are used.

2.2 Evolutionary strategies

The optimization algorithm finds the optimal pulse form for maximal ion yield by iteratively writing phase pattern onto the SLM according to the experimental feedback. A requirement for the optimization algorithm is to find global solutions in very high dimensional searching spaces. Additionally, the algorithm needs to be robust against experimental noise. It has been shown by Rabitz *et al.*, that indeterministic, random search strategies like Genetic Algorithms (GA) or Evolutionary Strategies (ES) are a good choice especially for experimental systems with high noise in the output side [20]. In this experiment we photoionize clusters within a molecular beam and use Evolutionary Strategies as the optimisation algorithm [21–23]. Evolutionary Strategies mimic the biological evolution. They employ operations like "cross-over", "mutation" and "survival-of-the-fittest". ES always try a number of possible solutions (called "individuals") until they proceed to the next iteration ("generation"). This ensemble of individuals is called "population". In the beginning of the cycle 10 parent individuals are created. Each individual is represented by an array of 128 random numbers between 0 and 2π, which specify the spectral phase shift. When sent to the modulator, a certain pulse shape is formed from a bandwidth-limited pulse. The cross-over operation creates 15 pairs of new individuals creates from randomly chosen pairs of parent individuals by randomly distributing their array elements between them. Thereby a

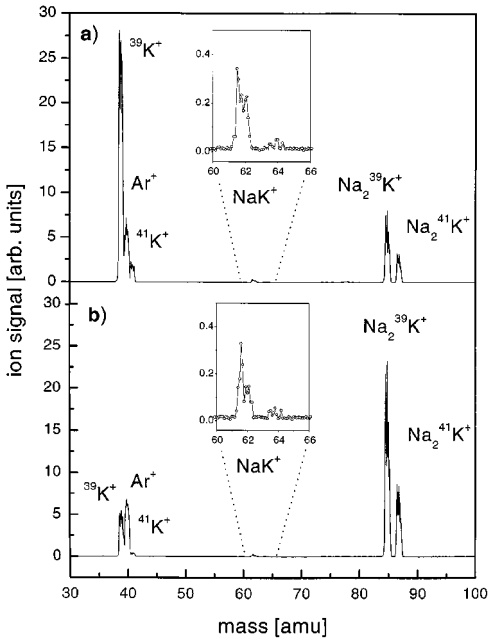

Fig. 3. Comparison of mass spectra obtained with a transform-limited pulse (a) and with the optimized pulse from Na_2K^+-yield optimization. The insets enlarge the NaK^+ peaks. The energies of the used pulses are equal in both cases.

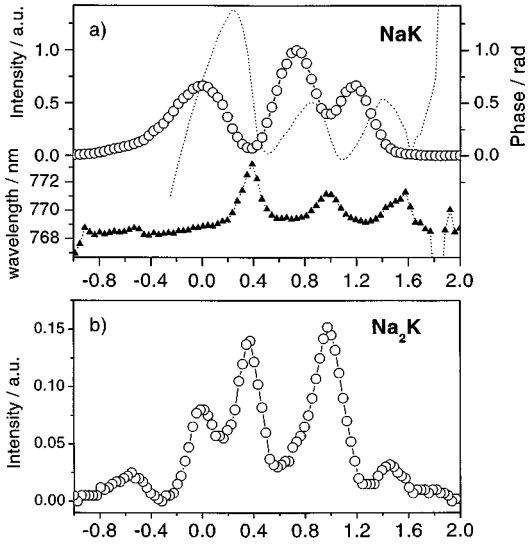

Fig. 4. Optimized pulse shapes for producing a maximum yield of (a) NaK^+ and (b) Na_2K^+. In (a) the pulse intensity is shown (circles) along with the temporal phase $\phi(t)$ (dotted line) and the chirp (triangles). In (b) the cross correlation trace of Na_2K^+ is plotted.

population of 30 individuals is formed. Each array element is then altered by adding a random number ("mutation leap") from a Gaussian probability distribution. This operation is called "mutation". The whole population is subsequently tested by recording the ion yield for each modulator setting. Only those 10 pulse shapes, which produce the highest ion yield are selected (survival of the fittest) and are taken as parents for the next generation. The optimization procedure proceeds until convergence of the ion yield is achieved. While cross-over operations only avoid the algorithm from getting trapped in a local minimum, mutation is the search operator. The mutation leap has to be set to the individual problem, which is accomplished by self-adaption.

3 Results and discussion

Figure 2 shows a typical trajectory of the ion yield of (a) NaK^+ and (b) Na_2K^+ during the optimization process. The pulses of the first generation have random phases. Consequently the pulses are very long and the ion signals weak. As the generations proceed, the algorithm enhances the ion signals by optimizing the phase of the laser pulse. Maximal gain was obtained after 65 and 145 generations for NaK^+ and Na_2K^+, respectively. While the trajectories and the number of generations needed to achieve convergence varied, the maximal yields were found to be almost the same. The ion yield gained with a short pulse is indicated in figure 2 with an arrow. For Na_2K the gain exceeds this level already after a few generations. This is shown in more detail in Figure 3. Two mass spectra of the mixed alkali cluster ions are shown, recorded with (a) a transform limited pulse and (b) the shaped pulse optimized for Na_2K^+ under the same experimental conditions and with the same laser power. As can be seen in figure 3, the intensity of the target cluster ion Na_2K^+ is enhanced by nearly a factor 3 compared to the reference spectrum. The K^+ peak decreases strongly while the Ar^+ intensity stays constant. The inset of figure 3 shows the NaK^+ peak. Compared with the transform-limited pulse, the pulse optimized for Na_2K^+ reduces the NaK^+ yield by about 40%. In the case of NaK, the optimization yields an enhancement of approximately 45%, compared with the reference spectrum, as indicated in Figure 2. The expansion conditions of the molecular beam were set as to produce more NaK and less higher clusters. Feedback optimized pulse shaping leads to a pronounced enhancement of ionic products. In the following the question will be addressed, if the pulse form leading to enhancement is carrying information about the physical processes involved.

3.1 NaK

In Figure 4a the pulse form of NaK^+ maximization is shown. From SHG FROG analysis a sequence of 3 pulses was retrieved. The central peak is about 70% higher than the other two and separated by $\Delta t = 690$ (± 20) fs and $\Delta t = 440$ (± 5) fs, respectively. The leading pulse in Figure 4a is considerably longer than the other two. Cross-correlation measurements indicate the time ordering of the pulse elements. Analysis of the temporal phase $\phi(t)$ of the pulse train reveals 4th order contribution in the first pulse and third order contributions in the others. The first derivative $\frac{\partial \phi(t)}{\partial t}$ gives the carrier frequency of the laser field. If $\phi(t)$ is of higher order, the carrier frequency is time

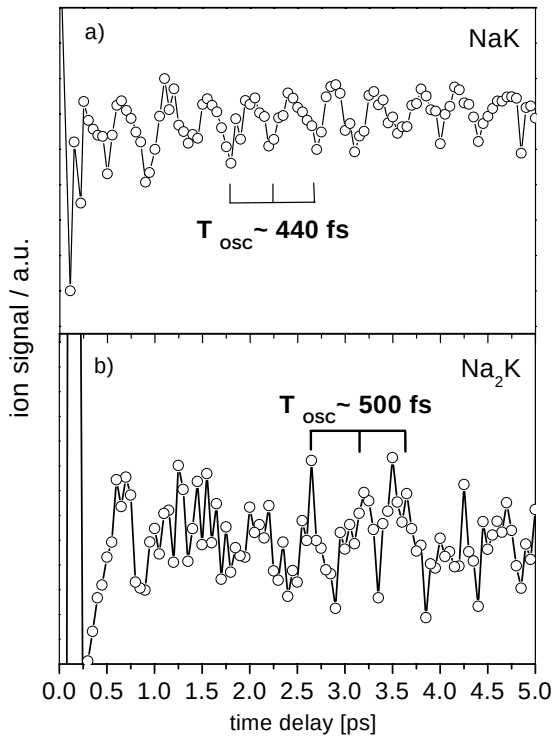

Fig. 5. Fs-pump-probe spectra of (a) NaK^+ and (b) Na_2K^+. For NaK^+ an oscillation period of 440 fs is obtained. In (b) the oscillatory component reveals a period of 500 fs for Na_2K^+. The exponential decay has been subtracted for clarification.

dependent, *i.e.* the pulse is chirped. In the lower part of figure 4a, the time dependent wavelength is plotted. The left pulse shows cubic down chirp, the other two quadratic down chirp. The intensity profile of the pulse train can be understood in the viewpoint of wave packet propagation. The pump-probe spectrum of the excited $^1A^+$-state of NaK at $\lambda_{pump} = \lambda_{probe} = 770$ nm reveals clear oscillations with a period of $\Delta t = 440$ fs (Figure 5a). The temporal separation between leading and central pulse of the optimal pulse form equals the duration of 1.5 oscillation periods in the pump-probe spectrum, while the other separation matches 1 oscillation period. The wavepacket is excited by the laser pulse in the inner turning point of the excited potential energy surface (PES). The second pulse hits the molecule after half integer oscillation periods. The wavepacket has propagated to the outer turning point of the PES, where the Franck-Condon factor for resonant 2-photon ionisation is higher [26]. The third pulse hits the molecule after another oscillation period, when the wavepacket is again located at the outer turning point of the PES. The intensity profile of the three pulses support the one-photon excitation and two-photon ionisation scheme. Due to anharmonicity of the potential energy surface the wavepacket disperses, leading to a smaller ionisation efficiency from the excited state. We find the first pulse stretched in time and down-chirped of third order. Down-chirped pump pulses can compensate for wavepacket dispersion. The blue spectral components excite vibrational levels of smaller spacing first, before higher frequencies are excited by the red components.

3.2 Na_2K

A cross-correlation trace of the pulse form after optimization of Na_2K^+ is shown in Figure 4b. It consists of three main peaks separated by 330 and 600 fs respectively, and two low-intensity peaks with a separation of about 500 fs. The first main pulse is about 60% lower than the other pulses. The interval between the first two pulses is about half the interval of second and third pulse. The first separation corresponds to 0.65 oscillation periods of the electronically excited trimer, and the interval between second and third pulse amounts about 1.2 oscillation periods (see the fs-pump-probe spectrum of Na_2K in Figure 5b). The separation to the weak pulses equals exactly the oscillation period. Vajda *et al.* have measured pump-probe multiphoton ionization spectra of Na_2K in the wavelength region between 730 and 790 nm [16]. They have found an oscillatory behaviour at the wavelength of 770 nm with a period of about 500 fs superimposed on a predissociation decay. As in the case of NaK, the oscillation is most likely due to the vibration of the excited Na_2K because the ion intensity reflects the time-dependent Franck-Condon factors between the excited and the ionization potentials. Like in the case of NaK, the three-pulse sequence can be explained as a pump pulse, which excites the trimer and creates a wave packet, and subsequent ionizing pulses, being timed with the wave packet located at the Franck-Condon favoured outer turning point. A detailed calculation on the wavepacket dynamics of alkali metal clusters is needed for the complete understanding of the pulse form, including the time mismatch of the main peaks and the contribution of the weak pulses.

4 Conclusion

We performed an adaptive feedback optimal control experiment on NaK and Na_2K clusters in a molecular beam. Optimization was achieved by enhancing the photoion yield of NaK^+ and Na_2K^+ by various magnitudes. The analysis of the optimized pulses show that the maximum intensity of the ion signals are obtained by a train of a few pulses separated by several vibrational periods. On complex surfaces of rather big molecules, solutions of non-intuitive forms are expected. In this experiment a system of intermediate complexity was chosen, where coherent dynamical behaviour could be observed. The feedback optimized solutions are partially understandable from the viewpoint of the wavepacket oscillation found in previous fs-pump-probe measurements. Multiphoton ionization and fragmentation are strongly enhanced by controlling the wavepackets of excited states according to the time dependent Franck-Condon-windows.

The authors thank Prof. H. Rabitz for stimulated discussions and Dr. T. Feurer and G. Stobrawa for the help and cooperation with the evolutionary algorithm. Prof. Dr. T. Leisner is

gratefully acknowledged for his helpful support in setting up the optimization method. One of the authors, C. Lupulescu, acknowledges the Gottlieb Daimler and Carl Benz-Stiftung for financial support. The present work is supported by the Deutsche Forschungsgemeinschaft (SFB 450).

References

1. R. de Vivie-Riedle, K. Kobe, J. Manz, W. Meyer, B. Reischel, S. Rutz, E. Schreiber, L. Wöste, J. Phys. Chem. **100**, 7789 (1996).
2. S. Rutz, S. Greschik, E. Schreiber, L. Wöste, Chem. Phys. Lett. **257**, 365 (1996).
3. E. Schreiber, K. Kobe, A. Ruff, S. Rutz, G. Sommerer, L. Wöste, Chem. Phys. Lett. **242**, 106 (1995).
4. A. Ruff, S. Rutz, E. Schreiber, L. Wöste, Z. Phys. D **37**, 175 (1996).
5. P. Brumer, M. Shapiro, Chem. Phys. Lett. **126**, 541 (1986).
6. P. Brumer, J. Hepburn, M. Shapiro, Chem. Phys. Lett. **149**, 451 (1988).
7. D. Tannor, S. Rice, J. Chem. Phys. **83**, 5013 (1985).
8. D. Tannor, R. Kosloff, S. Rice, J. Chem. Phys. **85**, 5805 (1986).
9. S. Shi, A. Woody, H. Rabitz, J. Chem. Phys. **88**, 6870 (1988).
10. A. Peirce, M. Dahleh, H. Rabitz, Phys. Rev. A **37**, 4950 (1988).
11. R. Kosloff, S. Rice, P. Gaspard, S. Tersigni, D. Tannor, Chem. Phys. **139**, 201 (1989).
12. W. Jakubetz, J. Manz, H.-J. Schreier, Chem. Phys. Lett. **165**, 100 (1990).
13. A. Weiner, D. Leaird, J. Patel, J. Wullert, IEEE J. Quant. Electr. **28**, 908 (1992).
14. R. Judson, H. Rabitz, Phys. Rev. Lett. **68**, 1500 (1992).
15. A. Assion, T. Baumert, M. Bergt, T. Brixner, B. Kiefer, V. Seyfried, M. Strehle, G. Gerber, Science **282**, 919 (1998).
16. S. Vajda, S. Rutz, J. Heufelder, P. Rosendo, H. Ruppe, P. Wetzel, L. Wöste, J. Phys. Chem. **102**, 4066 (1998).
17. M Wefer, K. Nelson, Opt. Lett. **20**, 1047 (1995).
18. M Wefer, K. Nelson, J. Opt. Soc. Am. B **12**, 1343 (1995).
19. O. Martinez, IEEE J. Quant. Electr. **24**, 2530 (1988).
20. G. Toth, A. Lörincz, H. Rabitz, J. Chem. Phys. **101**, 3715 (1994).
21. E. Schöneburg, F. Heinzmann, S. Feddersen, *Genetische Algorithmen und Evolutionsstrategien* (Addison-Wesley, Munich, 1994), p. 141.
22. I. Rechenberg, *Evolutionsstrategie* (Frommann-Hozboog, Stuttgart, 1994).
23. H.-P. Schwefel, *Evolution anf Optimum Seeking* (Wiley, New York, 1995).
24. R. Trebino, K.W. DeLong, D.N. Fittinghof, J.N. Sweetser, M.A. Krumbügel, B.A. Richman, D.J. Kane, Rev. Sci. Instrum **68**, 3277 (1997).
25. FROG 3.0, Femtosoft Technologies.
26. J. Heufelder, H. Ruppe, S. Rutz, E. Schreiber, L. Wöste, Chem. Phys. Lett. **269**, 1 (1997).